British Medical Bulletin, 2016, 1–11
doi: 10.1093/bmb/ldw049

Invited Review

Functional assessment of thoracic aortic aneurysms – the future of risk prediction?

Pouya Youssefi[†,‡], Rajan Sharma[†], C. Alberto Figueroa[‡,§], and Marjan Jahangiri[†,*]

[†]Department of Cardiothoracic Surgery & Cardiology, St. George's Hospital, St. George's University of London, Blackshaw Road, London, SW17 0QT, United Kingdom, [‡]Department of Biomedical Engineering, Rayne Institute, St. Thomas' Hospital, King's College London, London SE1 7EH, United Kingdom, and [§]Departments of Surgery and Biomedical Engineering, University of Michigan, Ann Arbor, MI 48109 USA

[*]Correspondence address. Department of Cardiothoracic Surgery, St. George's Hospital, Blackshaw Road, London SW17 0QT, United Kingdom. E-mail: marjan.jahangiri@stgeorges.nhs.uk

Editorial Decision 31 October 2016; Accepted 13 December 2016

Abstract

Introduction: Treatment guidelines for the thoracic aorta concentrate on size, yet acute aortic dissection or rupture can occur when aortic size is below intervention criteria. Functional imaging and computational techniques are a means of assessing haemodynamic parameters involved in aortic pathology.

Sources of data: Original articles, reviews, international guidelines.

Areas of agreement: Computational fluid dynamics and 4D flow MRI allow non-invasive assessment of blood flow parameters and aortic wall biomechanics.

Areas of controversy: Aortic valve morphology (particularly bicuspid aortic valve) is associated with aneurysm of the ascending aorta, although the exact mechanism of aneurysm formation is not yet established.

Growing points: Haemodynamic assessment of the thoracic aorta has highlighted parameters which are linked with both clinical outcome and protein changes in the aortic wall. Wall shear stress, flow displacement and helicity are elevated in patients with bicuspid aortic valve, particularly at locations of aneurysm formation.

Areas timely for developing research: With further validation, functional assessment of the aorta may help identify patients at risk of aortic

complications, and introduce new haemodynamic indices into management guidelines.

Key words: aorta, dissection, aortic valve, computational fluid dynamics, MRI, wall shear stress

Clinical need for functional assessment

For many years, size has been the principle decision-making criteria for intervention on the thoracic aorta.[1,2] Guidelines for the treatment of aortic disease concentrate on maximal aortic diameter and risk factors for dissection. Surgical replacement of the aorta is recommended when the aortic size reaches 55 mm, with earlier intervention recommended in the presence of connective tissue disorders (45 mm) or bicuspid aortic valve (BAV) (50 mm) when risk factors are present.[1] These risk factors include family history of acute aortic syndrome (aortic dissection, rupture or intramural haematoma), rapidly increasing aortic size and coarctation.

Yet despite these guidelines, there still remains a significant incidence of acute aortic events in patients whose aortas are smaller than these intervention thresholds. Elefteriades *et al.* found that in patients with aortic size below 50 mm, there still remains an incremental yearly risk of rupture, dissection or death above 5%.[3] These results were supported by data from the International Registry for Acute Aortic Dissections (IRAD), which showed that the highest incidence of acute aortic dissections occur at aortic size 50–54 mm, which falls below the standard size criteria of 55 mm for surgical intervention.[4] Furthermore, they showed that more aortic dissections occur when the aorta is sized 40–49 mm, as compared to 55–64 mm.

These datasets indicate that current intervention guidelines for management of the thoracic aorta may not be fully adequate in preventing acute complications. They suggest further information about the patient's individual aorta beyond size may be necessary to better predict aortic events and plan timing of intervention. As yet, there is no functional assessment of the thoracic aorta.

There is growing evidence that aortic valve morphology may be linked with aortopathy. BAV is the most common cardiac congenital abnormality, affecting 2% of the population. The morbidity and mortality related to BAV disease accounts for more than that related to all other congenital cardiac diseases combined.[5] BAV has been linked with aneurysms of the ascending aorta, with an associated risk of acute aortic complications such as dissection and rupture.[6] There is still controversy regarding the pathogenesis of dilatation of the aorta in BAV patients. Two main theories exist to explain aortic aneurysms in BAV patients: (1) genetic theory, where aortic wall weakness is a result of the common genetic developmental defect affecting both the aortic valve and the aortic wall; and (2) haemodynamic theory, where turbulent flow and eccentric jets caused by BAV leads to abnormal haemodynamic stress on the aortic wall and subsequently to aortopathy. The haemodynamic theory has gained strong support with recent advances in functional imaging.

Currently, a number of challenges face the cardiac surgeon and cardiologist in assessing and managing patients with thoracic aortic aneurysms. One challenge is deciphering which patients with aortic dilatation are likely to rupture or dissect imminently. Two very different patients may both present with an aortic size of 50 mm, yet one may have a stable aortic wall with low chance of dissection, and the other may have an area of aortic wall which is very thin with impending rupture or dissection. At this time, there is no formalized method of distinguishing between these two aortas. Another grey area for decision-making is whether to replace a moderately dilated ascending aorta when surgically intervening on the aortic valve, to prevent future surgery if the aorta dilates above size criteria for surgery. BAVs are associated with aortic aneurysms, however, we have shown no significant dilatation of the remaining ascending aorta or arch

after BAV/root replacement at 5-year follow-up.[7] The difficulties in decision-making and management of these patients would be made easier if more information is available about each individual's aortic haemodynamics and its effects on aortic pathology.

Modalities of haemodynamic assessment

To functionally assess the thoracic aorta, detailed haemodynamic measurements are required to investigate a variety of flow characteristics and biomechanical forces. However, measurement of *in-vivo* haemodynamics can be difficult and invasive.[8] Detailed anatomical imaging with assessment of flow and velocities enables calculation of physiological parameters without the need for invasive monitoring.

Computational fluid dynamics

Computational fluid dynamics (CFD) is an ever increasing approach to quantify haemodynamics in high spatial and temporal resolution.[9,10] Computational simulations of blood flow can be used in the study of aortic wall biomechanics, as well as blood flow characteristics which may be involved in aortic disease processes. CFD has been applied in assessment of aneurysms and rupture risk,[11–13] the design and assessment of vascular devices,[14,15] and the planning and outcome prediction of vascular surgeries.[16–18]

Imaging & modelling

In order to perform CFD simulations, detailed anatomical imaging is required to create accurate 3D geometric models of the thoracic aorta. Imaging modalities such as Cardiovascular Magnetic Resonance Imaging (CMR) or multi-slice CT may be used to acquire the anatomical data. In the case of CMR, aortic anatomy can be visualized either using angiography (MR Angiography) where intravenous contrast is injected, or through high-resolution cardiac and respiratory gated 3D steady state in free precession (SSFP). In the case of MR Angiography, the contrast load is usually less nephrotoxic than that used in CT Angiography. CT Angiography may also be carried out with Electrocardiogram (ECG)-gating in order to reduce motion artefact.

Geometric models of the aorta are reconstructed by segmenting the imaging data. The vessel segmentation procedure is carried out by identifying the vessel boundary through thresholding, where differences in pixel intensity are used to automatically detect vessel boundaries, or by manual interaction. An automated lofting process then interpolates all segmented boundaries thus creating the 3D model of the aorta and its branches. The geometric model is then used to create a detailed mesh of the aorta. It is at the grid-points throughout this mesh where haemodynamic variables such as velocity, stress and pressure are calculated. Therefore, the mesh may be made to be finer near the vessel wall, in order to provide more data points in regions of interest (Fig. 1).[19]

Boundary conditions

The geometric mesh of the aorta provides the framework of data points (or nodes) at which haemodynamic calculations can be made. In order for blood flow CFD simulations to be carried out, conditions have to be imposed at the inlet of the aorta (i.e. the aortic root) as well as the outlet of each branch of the aorta (for e.g. the head and neck vessels and descending thoracic aorta). A key aspect in the endeavour of accurate CFD simulations is the specification of physiologically accurate boundary conditions.[9,20–26]

Up until recently, many studies used idealized velocity profiles for the inflow boundary conditions. Such studies have modelled inflow boundary conditions using simple profiles (such as a parabolic or Womersley).[27] This has been shown to have a significant effect on haemodynamic calculations further along the aorta.[28] However, the aortic valve is a complex trileaflet structure, and in union with the sinuses of Valsalva and coronary arteries which make up the aortic root, leads to intricate flow patterns entering the ascending aorta.[29] These flow patterns are much more complex than the simple idealized profiles. Furthermore, an array of pathologies may affect the

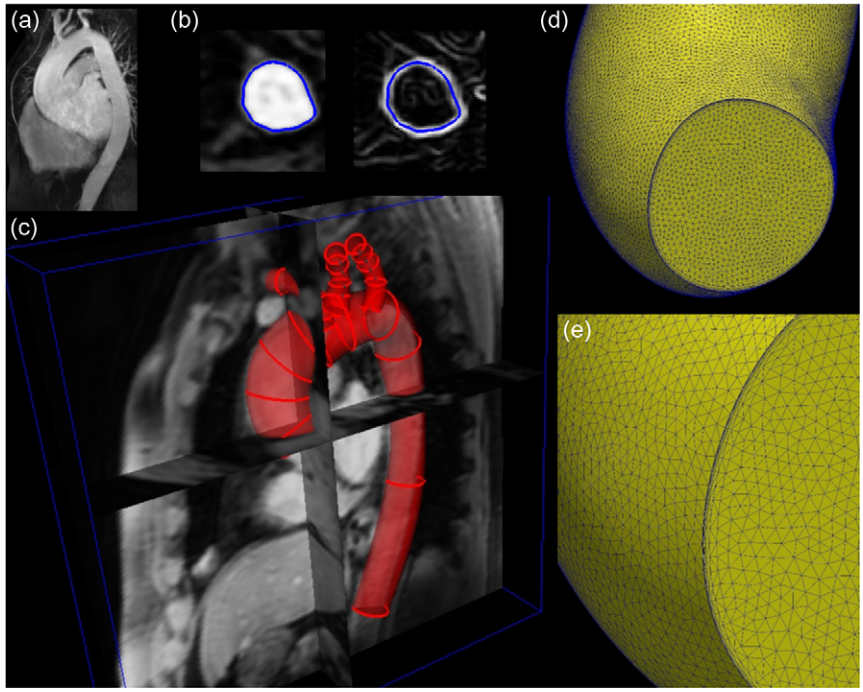

Fig. 1 (**a**) MR Angiogram of the thoracic aorta; (**b**) segmentation of the boundary of the aorta through thresholding, in which differences in pixel intensity are used to detect vessel boundaries; (**c**) all segmented boundaries (shown in red rings) are automatically lofted to create the aorta model; (**d**) tetrahedral mesh of the thoracic aorta; and (**e**) the mesh is refined at the wall boundary to allow for more data points to be analysed at the region of interest: the aortic wall.

aortic valve, including stenosis, regurgitation, and importantly the congenital malformation causing the valve to be bicuspid.[30,31] Therefore, there is a need to apply accurate patient-specific inflow boundary conditions to CFD simulations of the thoracic aorta in order to achieve meaningful haemodynamic measurements.

CMR allows flow measurement using phase-contrast (PC-MRI) techniques by means of gradient echo sequences. This measures blood flow and velocity at a given plane along the aorta. If measured at or above the aortic valve, these flow measurements can be used to assign an inlet velocity profile into the aortic model, thereby forming the inlet boundary condition for CFD simulations (Fig. 2).

The anatomical mesh and boundary conditions are then fed into a computational solver where blood flow simulations are carried out to solve a set of equations (e.g. Navier–Stokes equations for blood flow) enforcing conservation of mass (continuity). This calculates the relevant haemodynamic variables throughout the aorta which can then be post-processed to analyse for different flow characteristics and biomechanical forces.

4D flow MRI

In flow MRI, phase-contrast methods are used to encode blood flow velocities along all dimensions. This permits acquisition of spatially registered flow data along with morphological data.[32] 4D flow MRI is the acquisition of 3D cine PC-MRI acquired in a time-resolved ECG-gated manner with three-directional velocity encoding. It allows post-hoc time-resolved 3D visualization along with quantification of flow at any location within a volume.[33] In addition to the acquisition of basic flow volumes and velocities, other haemodynamic measurements can also be calculated, as discussed later. Some of these haemodynamic measurements relating to flow

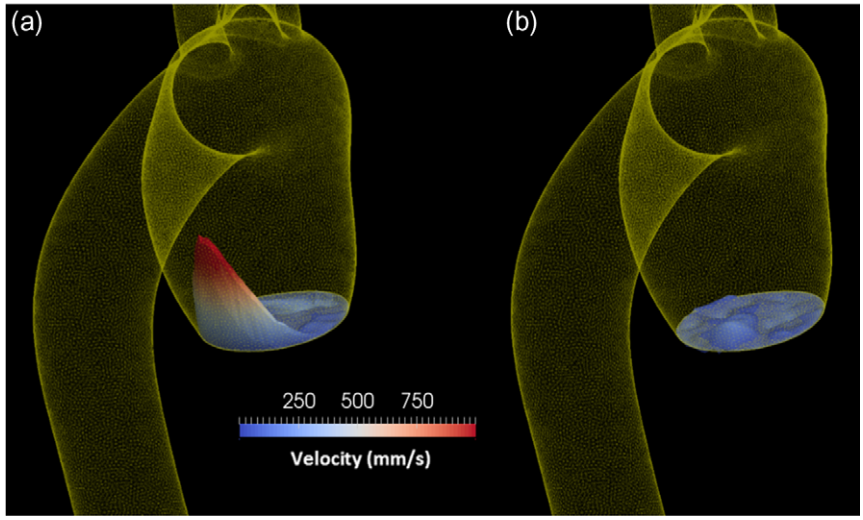

Fig. 2 Inflow velocity profile mapped onto the inlet of the aorta mesh; (**a**) peak systole where an eccentric jet is seen at the periphery of the lumen; and (**b**) late diastole.

and velocity are the same as those calculated using CFD.

Comparison of CFD and 4D flow MRI

One of the challenges of 4D flow MRI is that the acquisition of velocity data in three dimensions can be time-consuming, meaning the patient has to undergo a longer scan time. Spatial resolution can be lower than CFD, and provides an ensemble-averaged haemodynamic assessment over several cardiac cycles.

On the other hand, CFD has no limit in temporal and spatial resolution. Furthermore, it also provides spatially-varying description of pressure indices (not just velocity). In the most sophisticated settings, CFD can also account for wall motion via fluid–structure interaction formulations.[8] The imaging time required to obtain aortic anatomical data for the geometric mesh, as well as the flow data (PC-MRI) above the aortic valve for the inflow boundary conditions, is much shorter in duration compared to 4D flow MRI. Therefore patients have to spend much less time in the MRI scanner. However, the subsequent blood flow simulations are computationally expensive and are of varying duration.

Whereas 4D flow MRI is limited to only acquiring live data from patients, CFD has the capacity to simulate proposed changes in anatomy and physiological parameters which may be the result of medical, surgical or pharmacological interventions, in order to see the effect that these may have on haemodynamics and biomechanics.[34–36] This allows simulating interventions and procedures to see their effects, without putting patients at the risks of the intervention.

Nevertheless, CFD and 4D flow MRI can be used together to further improve understanding of hemodynamics in aortic disease. They are different experimental techniques, with different strengths and weaknesses.

Haemodynamic parameters & clinical implications

Disease processes such as aneurysm formation and atherosclerosis are largely dependent on haemodynamic factors in the vascular system.[37–40] Flow characteristics play an important role in this disease process, with effects on endothelial homeostasis[41,42] and response of smooth muscle cells and fibroblasts.[41,43–45]

Wall shear stress

Wall shear stress (WSS) refers to the force per unit area exerted by a moving fluid in the direction of

that vessel.[46] According to the Newtonian incompressible fluid approximation, WSS depends on the dynamic viscosity μ of the fluid, and the velocity gradient near the vessel wall, namely the wall shear rate (WSR):

$$\mathrm{WSS} = \mu \mathrm{WSR} = \mu \frac{\mathrm{d}u}{\mathrm{d}r}$$

where WSS is measured in pressure units (dyn/cm^2), μ is the dynamic viscosity of blood, measured in Poise, du/dr is the velocity gradient of the blood which is called Shear Rate (SR), measured in s^{-1}. When considering the vessel wall, this gradient is the WSR. WSR is a measure of the rate of velocity increase when moving away from the vessel wall (where according to the no slip condition the velocity is zero).

WSS was first associated with vasculopathy in the context of plaque formation. Gnasso *et al.* observed that WSS was lower in those carotid arteries which had higher levels of plaque formation.[47] Furthermore, a correlation was found between low WSS and an increase in the intima-media thickness of carotid arteries.[48] Malet *et al.* described how WSS <4 dyn/cm^2 stimulates an atherogeneric phenotype, whereas a level >15 dyn/cm^2 induces endothelial quiescence and an atheroprotective gene expression profile.[49]

Subsequently, focus has turned to the link between high WSS and aneurysm formation. This was first reported in the cerebral circulation. Cebral *et al.* assessed rupture sites of cerebral aneurysms and found that they correlated with areas of high WSS.[50] In turn, WSS in the thoracic aorta has been the recent subject of intense research, particularly in the context of aortic valve-related aortopathy. Barker *et al.* found that WSS in the ascending aorta of patients with BAV was significantly elevated compared to healthy volunteers.[51] BAV with fusion of the right and non-coronary cusps was shown to have higher WSS and larger ascending aorta size.[52] The ascending aorta is the commonest site of aneurysm formation in BAV. Mahadevia *et al.* further sub-analysed regional WSS distribution in circumferential sub-sectors of the ascending aorta of patients with BAV compared to tricuspid aortic valve (TAV).[53] They found elevated WSS in the right-anterior wall of the ascending aorta for right-left fusion BAV, and right-posterior wall for right-non fusion BAV. These regions correspond to the greater curvature of the ascending aorta, the typical site of dilatation in BAV-related aortopathy (Fig. 3).

The trend that WSS is elevated in the greater curvature of BAV aortas correlates well with the findings of Della Corte *et al.* who found that medial degeneration was more severe in this region.[54] Type I and III collagen were reduced, and smooth muscle cell apoptosis was seen to be increased in the greater curvature even before significant dilatation had occurred.[55] An important recent study by Guzzardi *et al.* has shown a direct link between WSS and changes in the wall of the ascending aorta.[56] BAV patients undergoing ascending aorta replacement had pre-operative WSS mapping. At the time of surgery, paired aortic wall samples were taken from regions of elevated WSS and normal WSS. They found increased transforming growth factor β-1, matrix metalloproteinase (MMP)-1, MMP-2 and MMP-3 in regions of high WSS, indicating extracellular

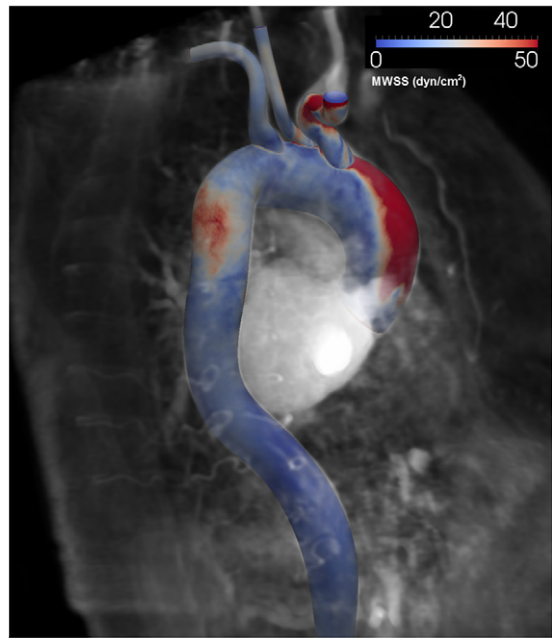

Fig. 3 Mean WSS (MWSS) map of the thoracic aorta showing high WSS in the greater curvature of the ascending aorta in a patient with BAV.

matrix dysregulation. Furthermore, there was higher medial elastin degradation in regions of high WSS. To support this finding, High WSS has also been associated with internal elastic lamina loss in basilar arteries.[57]

High WSS may thus promote a series of responses which produce thinning of the aortic wall, and in doing so contribute to aneurysm formation. This may help to explain why some patients with aortic size below current intervention criteria develop acute aortic complications.

Flow patterns

Flow patterns in the thoracic aorta differ significantly depending on aortic valve morphology. Flow profiles exiting the aortic root for healthy TAV show broad centrally distributed jets, whereas in BAV there is asymmetry with higher velocity jets at the periphery near the aortic wall. The flow angle of blood exiting the aortic valve is elevated in BAV, and flow displacement (a measure of flow eccentricity) is consistent with differences in regionally increased ascending aorta WSS.[53]

Velocity streamlines help to visualize the direction of flow at any given time in the cardiac cycle. Streamlines are tangent to the velocity vector, and show the direction in which a fluid element will travel at any point in time. Healthy TAV produce laminar flow patterns with parallel streamlines indicating flow in line with the aortic wall. In contrast, velocity streamlines in BAV show eccentric jets with disrupted patterns, loss of laminar flow, and impingement of flow at the greater curvature (Fig. 4).[53]

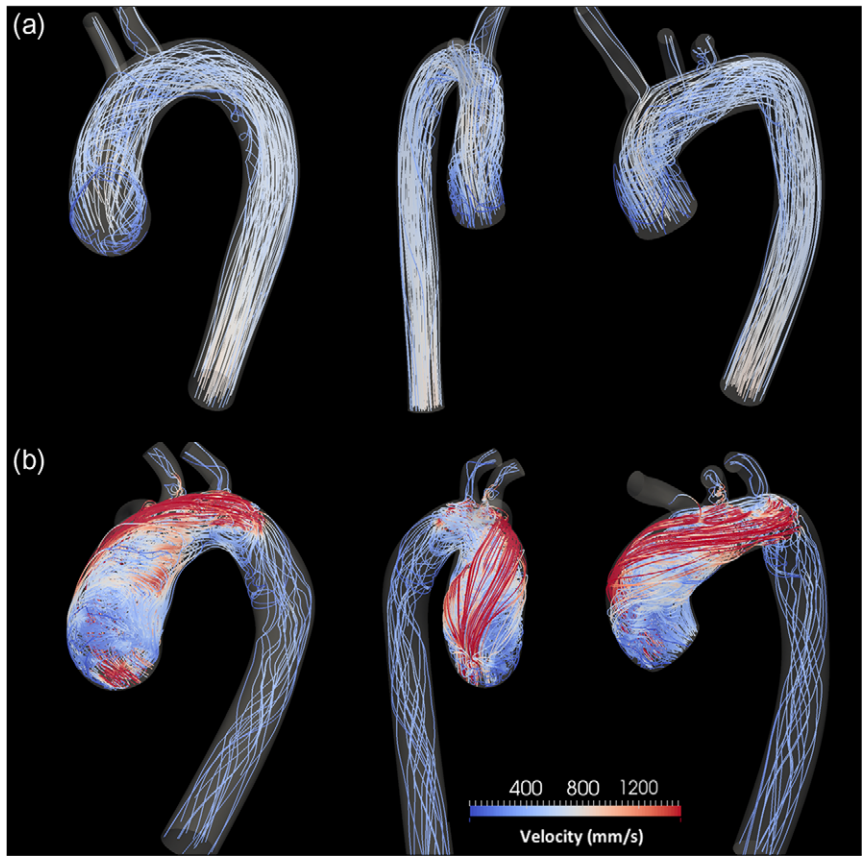

Fig. 4 Velocity streamlines during systole; (**a**) healthy volunteer showing parallel streamlines indicating undisrupted flow and (**b**) bicuspid aortic valve patient showing high velocity jet impinging on the greater curvature of the ascending aorta, with highly helical flow patterns.

Helical flow

It is increasingly recognized that flow in the thoracic aorta contains significant radial (non-axial) components associated with helical flow.[58] This is due to a combination of factors including ventricular twist and torsion during systole,[59,60] the fluid mechanics of the aortic valve and aortic root,[61] and the curved morphology of the ascending, arch and descending aorta.[62–65] From a physiological viewpoint, helical flow may be beneficial and/or detrimental. It may comprise a degree of normal organ perfusion.[66] On the other hand, it has been shown to play an important role in plaque deposition.[67] Pritchard *et al.* demonstrated differences in monocyte adhesion to the vascular wall (important cells in the pathogenesis of atherosclerotic plaques) related to the radial component of velocity.[68]

Bissell *et al.* compared helical flow patterns in BAV and TAV patients.[52] They found BAV was associated with abnormal right-handed helical flow, which correlated with higher rotational helical flow, higher WSS and larger ascending aortas. BAV with right-non cusp fusion and right-handed flow showed the most severe flow abnormalities. On the other hand, patients with BAV who had normal flow patterns elicited WSS and aortic dimensions comparable to healthy volunteers.[52]

Future applications

CFD and 4D flow MRI provide sophisticated non-invasive methods of acquiring haemodynamic data in the thoracic aorta. They have the potential to predict complications and prognosis of these diseases, as well as introduce new indices (such as WSS) into management guidelines for the aorta and the aortic valve. For this to happen, validation of these haemodynamic indices will be required.

One form of validation will be proof that these haemodynamic parameters are linked to pathological changes in the aortic wall. As mentioned earlier, recent studies have already shown that high WSS is linked to loss of elastin, as well as disruption of extracellular matrix proteins.[56] Further work to acquire detailed knowledge of these protein pathways and their association with aneurysm formation is required. Moreover, *in-vitro* studies with control over applied flow parameters to aortic wall tissue will be able to assess these links with more accuracy and less confounding factors.

To fully acquire clinical relevance, longitudinal studies will be required to look at the long-term effects of these haemodynamic parameters on clinical outcomes. Patients who undergo functional imaging with measurement of these haemodynamic indices can subsequently be monitored by routine clinical assessment and imaging. These can include serial measurements of aortic size, as well as the development of acute aortic events. These studies are already under way and will likely be most significant in implementing functional assessment of the aorta into routine clinical practice.

Future applications for functional imaging of the aorta may involve the assessment and comparison of interventions on the aorta and the aortic valve. Analysis of haemodynamics following surgical aortic valve replacement and comparison with transcatheter aortic valve implantation (TAVI) may shed light on their role in aortic pathophysiology (whether pre-existing or de-novo). Furthermore, assessment following aortic valve repair procedures (including valve-sparing aortic root replacement) may provide indicators for the long-term durability of the technique.

Conclusions

The spectrum of aortic disease is varied and complex. Aortic size alone does not distinguish between different pathological processes which vary in their risk of acute complications. Traditional guidelines for the aorta, which focus on maximal aortic diameter, have remained largely unchanged for many years. Data from epidemiological studies and registries indicate acute aortic dissection or rupture can occur when the aortic size is below intervention criteria. This has highlighted the need to develop functional assessment of the thoracic aorta in order to understand the haemodynamic causes for aortopathy, as well as a means of better predicting complications. CFD and 4D flow MRI provide a potential

method of acquiring this functional assessment, and with development and validation may prove to be the game-changer in the management of aortic disease.

Acknowledgements

This work was supported by the European Research Council under the European Union's Seventh Framework Programme FP/2007-2013/European Research Council (Grant Agreement no. 307532 to A.F.), British Heart Foundation New Horizons programme (NH/11/5/29058 to A.F.), the Royal College of Surgeons of England Research Fellowship (to P.Y.), the United Kingdom Department of Health via the National Institute for Health Research (NIHR) comprehensive Biomedical Research Centre award to Guy's & St Thomas' NHS Foundation Trust in partnership with King's College London and King's College Hospital NHS Foundation Trust.

Conflict of interest statement

The authors have no potential conflicts of interest.

References

1. Erbel R, Aboyans V, Boileau C, et al. 2014 ESC Guidelines on the diagnosis and treatment of aortic diseases: Document covering acute and chronic aortic diseases of the thoracic and abdominal aorta of the adult. The task force for the diagnosis and treatment of aortic diseases of the European Society of Cardiology (ESC). *Eur Heart J* 2014;35:2873–926.
2. Svensson LG, Adams DH, Bonow RO, et al. Aortic valve and ascending aorta guidelines for management and quality measures. *Ann Thorac Surg* 2013;95:S1–66.
3. Elefteriades JA, Farkas EA. Thoracic aortic aneurysm clinically pertinent controversies and uncertainties. *J Am Coll Cardiol* 2010;55:841–57.
4. Pape LA, Tsai TT, Isselbacher EM, et al. Aortic diameter > or = 5.5 cm is not a good predictor of type A aortic dissection: observations from the International Registry of Acute Aortic Dissection (IRAD). *Circulation* 2007;116:1120–7.
5. Ward C. Clinical significance of the bicuspid aortic valve. *Heart* 2000;83:81–5.
6. Della Corte A, Bancone C, Quarto C, et al. Predictors of ascending aortic dilatation with bicuspid aortic valve: a wide spectrum of disease expression. *Eur J Cardiothorac Surg* 2007;31:397–404. discussion 404–5.
7. Abdulkareem N, Soppa G, Jones S, et al. Dilatation of the remaining aorta after aortic valve or aortic root replacement in patients with bicuspid aortic valve: a 5-year follow-up. *Ann Thorac Surg* 2013;96:43–9.
8. Xiong G, Figueroa CA, Xiao N, et al. Simulation of blood flow in deformable vessels using subject-specific geometry and spatially varying wall properties. *Int J Numer Method Biomed Eng* 2011;27:1000–16.
9. Milner JS, Moore JA, Rutt BK, et al. Hemodynamics of human carotid artery bifurcations: computational studies with models reconstructed from magnetic resonance imaging of normal subjects. *J Vasc Surg* 1998; 28:143–56.
10. Cebral JR, Yim PJ, Lohner R, et al. Blood flow modeling in carotid arteries with computational fluid dynamics and MR imaging. *Acad Radiol* 2002;9: 1286–99.
11. Fillinger MF, Raghavan ML, Marra SP, et al. In vivo analysis of mechanical wall stress and abdominal aortic aneurysm rupture risk. *J Vasc Surg* 2002;36:589–97.
12. Fillinger MF, Marra SP, Raghavan ML, et al. Prediction of rupture risk in abdominal aortic aneurysm during observation: wall stress versus diameter. *J Vasc Surg* 2003;37:724–32.
13. Les AS, Shadden SC, Figueroa CA, et al. Quantification of hemodynamics in abdominal aortic aneurysms during rest and exercise using magnetic resonance imaging and computational fluid dynamics. *Ann Biomed Eng* 2010;38:1288–313.
14. Li Z, Kleinstreuer C. Blood flow and structure interactions in a stented abdominal aortic aneurysm model. *Med Eng Phys* 2005;27:369–82.
15. Stuhne GR, Steinman DA. Finite-element modeling of the hemodynamics of stented aneurysms. *J Biomech Eng* 2004;126:382–7.
16. Migliavacca F, Balossino R, Pennati G, et al. Multiscale modelling in biofluidynamics: application to reconstructive paediatric cardiac surgery. *J Biomech* 2006;39: 1010–20.
17. Soerensen DD, Pekkan K, de Zelicourt D, et al. Introduction of a new optimized total cavopulmonary connection. *Ann Thorac Surg* 2007;83:2182–90.
18. Taylor CA, Draney MT, Ku JP, et al. Predictive medicine: computational techniques in therapeutic decision-making. *Comput Aided Surg* 1999;4:231–47.
19. Torii R, Xu XY, El-Hamamsy I, et al. Computational biomechanics of the aortic root. *Aswan Heart Cent Sci Pract Ser* 2011;2011:16.
20. Lee SW, Steinman DA. On the relative importance of rheology for image-based CFD models of the carotid bifurcation. *J Biomech Eng* 2007;129:273–8.

21. Lee KW, Wood NB, Xu XY. Ultrasound image-based computer model of a common carotid artery with a plaque. *Med Eng Phys* 2004;26:823–40.
22. Steinman DA. Image-based computational fluid dynamics modeling in realistic arterial geometries. *Ann Biomed Eng* 2002;30:483–97.
23. Wake AK, Oshinski JN, Tannenbaum AR, et al. Choice of in vivo versus idealized velocity boundary conditions influences physiologically relevant flow patterns in a subject-specific simulation of flow in the human carotid bifurcation. *J Biomech Eng* 2009;131:021013.
24. Moyle KR, Antiga L, Steinman DA. Inlet conditions for image-based CFD models of the carotid bifurcation: is it reasonable to assume fully developed flow? *J Biomech Eng* 2006;128:371–9.
25. Steinman DA, Thomas JB, Ladak HM, et al. Reconstruction of carotid bifurcation hemodynamics and wall thickness using computational fluid dynamics and MRI. *Magn Reson Med* 2002;47:149–59.
26. Vignon-Clementel IE, Figueroa CA, Jansen KE, et al. Outflow boundary conditions for 3D simulations of non-periodic blood flow and pressure fields in deformable arteries. *Comput Methods Biomech Biomed Engin* 2010;13:625–40.
27. Campbell IC, Ries J, Dhawan SS, et al. Effect of inlet velocity profiles on patient-specific computational fluid dynamics simulations of the carotid bifurcation. *J Biomech Eng* 2012;134:051001.
28. Nakamura M, Wada S, Yamaguchi T. Computational analysis of blood flow in an integrated model of the left ventricle and the aorta. *J Biomech Eng* 2006;128:837–43.
29. Sigovan M, Dyverfeldt P, Wrenn J, et al. Extended 3D approach for quantification of abnormal ascending aortic flow. *Magn Reson Imaging* 2015;33:695–700.
30. Waller BF, Howard J, Fess S. Pathology of aortic valve stenosis and pure aortic regurgitation: a clinical morphologic assessment–Part II. *Clin Cardiol* 1994;17:150–6.
31. Waller B, Howard J, Fess S. Pathology of aortic valve stenosis and pure aortic regurgitation. A clinical morphologic assessment–Part I. *Clin Cardiol* 1994;17:85–92.
32. Markl M, Schnell S, Wu C, et al. Advanced flow MRI: emerging techniques and applications. *Clin Radiol* 2016;71:779–95.
33. Markl M, Frydrychowicz A, Kozerke S, et al. 4D flow MRI. *J Magn Reson Imaging* 2012;36:1015–36.
34. LaDisa JF Jr., Dholakia RJ, Figueroa CA, et al. Computational simulations demonstrate altered wall shear stress in aortic coarctation patients treated by resection with end-to-end anastomosis. *Congenit Heart Dis* 2011;6:432–43.
35. Prasad A, Xiao N, Gong XY, et al. A computational framework for investigating the positional stability of aortic endografts. *Biomech Model Mechanobiol* 2013;12:869–87.
36. Figueroa CA, Taylor CA, Yeh V, et al. Effect of curvature on displacement forces acting on aortic endografts: a 3-dimensional computational analysis. *J Endovasc Ther* 2009;16:284–94.
37. Friedman MH, Hutchins GM, Bargeron CB, et al. Correlation between intimal thickness and fluid shear in human arteries. *Atherosclerosis* 1981;39:425–36.
38. Zarins CK, Giddens DP, Bharadvaj BK, et al. Carotid bifurcation atherosclerosis. Quantitative correlation of plaque localization with flow velocity profiles and wall shear stress. *Circ Res* 1983;53:502–14.
39. Yeung JJ, Kim HJ, Abbruzzese TA, et al. Aortoiliac hemodynamic and morphologic adaptation to chronic spinal cord injury. *J Vasc Surg* 2006;44:1254–65.
40. Humphrey JD, Taylor CA. Intracranial and abdominal aortic aneurysms: similarities, differences, and need for a new class of computational models. *Annu Rev Biomed Eng* 2008;10:221–46.
41. Chien S, Li S, Shyy YJ. Effects of mechanical forces on signal transduction and gene expression in endothelial cells. *Hypertension* 1998;31:162–9.
42. Davies PF. Flow-mediated endothelial mechanotransduction. *Physiol Rev* 1995;75:519–60.
43. Gibbons GH, Dzau VJ. The emerging concept of vascular remodeling. *N Engl J Med* 1994;330:1431–8.
44. Langille BL. Arterial remodeling: relation to hemodynamics. *Can J Physiol Pharmacol* 1996;74:834–41.
45. Humphrey JD. Mechanisms of arterial remodeling in hypertension: coupled roles of wall shear and intramural stress. *Hypertension* 2008;52:195–200.
46. Efstathopoulos EP, Patatoukas G, Pantos I, et al. Wall shear stress calculation in ascending aorta using phase contrast magnetic resonance imaging. Investigating effective ways to calculate it in clinical practice. *Phys Med* 2008;24:175–81.
47. Gnasso A, Irace C, Carallo C, et al. In vivo association between low wall shear stress and plaque in subjects with asymmetrical carotid atherosclerosis. *Stroke* 1997;28:993–8.
48. Gnasso A, Carallo C, Irace C, et al. Association between intima-media thickness and wall shear stress in common carotid arteries in healthy male subjects. *Circulation* 1996;94:3257–62.
49. Malek AM, Alper SL, Izumo S. Hemodynamic shear stress and its role in atherosclerosis. *JAMA* 1999;282:2035–42.

50. Cebral JR, Vazquez M, Sforza DM, et al. Analysis of hemodynamics and wall mechanics at sites of cerebral aneurysm rupture. *J Neurointerv Surg* 2015;7:530–6.
51. Barker AJ, Markl M, Burk J, et al. Bicuspid aortic valve is associated with altered wall shear stress in the ascending aorta. *Circ Cardiovasc Imaging* 2012;5:457–66.
52. Bissell MM, Hess AT, Biasiolli L, et al. Aortic dilation in bicuspid aortic valve disease: flow pattern is a major contributor and differs with valve fusion type. *Circ Cardiovasc Imaging* 2013;6:499–507.
53. Mahadevia R, Barker AJ, Schnell S, et al. Bicuspid aortic cusp fusion morphology alters aortic three-dimensional outflow patterns, wall shear stress, and expression of aortopathy. *Circulation* 2014;129:673–82.
54. Della Corte A, De Santo LS, Montagnani S, et al. Spatial patterns of matrix protein expression in dilated ascending aorta with aortic regurgitation: congenital bicuspid valve versus Marfan's syndrome. *J Heart Valve Dis* 2006;15:20–7. discussion 27.
55. Della Corte A, Quarto C, Bancone C, et al. Spatiotemporal patterns of smooth muscle cell changes in ascending aortic dilatation with bicuspid and tricuspid aortic valve stenosis: focus on cell-matrix signaling. *J Thorac Cardiovasc Surg* 2008;135:8–18. 18.e1–2.
56. Guzzardi DG, Barker AJ, van Ooij P, et al. Valve-related hemodynamics mediate human bicuspid aortopathy: insights from wall shear stress mapping. *J Am Coll Cardiol* 2015;66:892–900.
57. Metaxa E, Tremmel M, Natarajan SK, et al. Characterization of critical hemodynamics contributing to aneurysmal remodeling at the basilar terminus in a rabbit model. *Stroke* 2010;41:1774–82.
58. Markl M, Draney MT, Hope MD, et al. Time-resolved 3-dimensional velocity mapping in the thoracic aorta: visualization of 3-directional blood flow patterns in healthy volunteers and patients. *J Comput Assist Tomogr* 2004;28:459–68.
59. Baciewicz FA, Penney DG, Marinelli WA, et al. Torsional ventricular motion and rotary blood flow. What is the clinical significance. *Cardiac Chronicle* 1991;5:1–8.
60. Farthing S, Peronneau P. Flow in the thoracic aorta. *Cardiovasc Res* 1979;13:607–20.
61. Bellhouse BJ, Reid KG. Fluid mechanics of the aortic valve. *Br Heart J* 1969;31:391.
62. Chandran KB. Flow dynamics in the human aorta. *J Biomech Eng* 1993;115:611–6.
63. Chandran KB, Yearwood TL, Wieting DW. An experimental study of pulsatile flow in a curved tube. *J Biomech* 1979;12:793–805.
64. Yearwood TL, Chandran KB. Experimental investigation of steady flow through a model of the human aortic arch. *J Biomech* 1980;13:1075–88.
65. Yearwood TL, Chandran KB. Physiological pulsatile flow experiments in a model of the human aortic arch. *J Biomech* 1982;15:683–704.
66. Frazin LJ, Vonesh MJ, Chandran KB, et al. Confirmation and initial documentation of thoracic and abdominal aortic helical flow. An ultrasound study. *ASAIO J* 1996;42:951–6.
67. Kilner PJ, Yang GZ, Mohiaddin RH, et al. Helical and retrograde secondary flow patterns in the aortic arch studied by three-directional magnetic resonance velocity mapping. *Circulation* 1993;88:2235–47.
68. Pritchard WF, Davies PF, Derafshi Z, et al. Effects of wall shear stress and fluid recirculation on the localization of circulating monocytes in a three-dimensional flow model. *J Biomech* 1995;28:1459–69.